

Structural Studies on the Titanium-Nitrogen System

BO HOLMBERG

Institute of Inorganic and Physical Chemistry, University of Stockholm, Stockholm, Sweden

The titanium-nitrogen system has been investigated by X-ray methods using samples quenched after annealing at 900°C. The solubility of nitrogen in α -titanium was found to be 17 at. % ($\text{TiN}_{0.20}$), the solid solutions having randomly distributed nitrogen atoms. The crystal structure of the so-called ε phase, which was found to occur within a narrow range of homogeneity at the composition $\text{TiN}_{0.50}$, has been determined. It is tetragonal, space-group $P4_2/mnm$, with a unit cell content of 2 Ti_2N and the unit cell dimensions $a = 4.9452 \text{ \AA}$ and $c = 3.0342 \text{ \AA}$. The structure is of an *anti*-rutile type. The lower limit of the homogeneity range of the TiN phase is at $\text{TiN}_{0.4}$.

In connection with structural studies on solid solutions of oxygen in *hcp* titanium, zirconium and hafnium ¹⁻³, it was found to be of interest to examine the titanium-nitrogen system. Previous work by Ehrlich ⁴ has revealed the existence of a wide range of solid solubility of nitrogen in α -titanium ($\text{TiN}_{0-0.22}$) and of the phase $\text{TiN}_{0.42-1}$ of a defective *B1* type of structure. Palty, Margolin and Nielsen ⁵ reported furthermore a phase (called ε) at a composition of about 26 at. % N with a tetragonal unit cell and suggested the formula to be either Ti_4N or Ti_3N . However, Nowotny, Benesovsky, Brukl and Schob ⁶ stated that the ε phase exists within a narrow range of homogeneity close to the composition $\text{TiN}_{0.5}$ and accordingly suggested the formula Ti_2N .

EXPERIMENTAL

The starting materials were titanium sponge (Johnson, Mathey and Co. Ltd., 99.98 % pure) and TiN prepared from the metal by heating it in a stream of purified nitrogen at 1250°C. The alloys were obtained by melting appropriate mixtures of the starting materials in an electric arc furnace under an argon atmosphere. Part of each melt was then crushed and annealed at 900°C in a sealed, evacuated silica tube for about a month. A tantalum foil protected the specimen from reacting with the silica. The heat-treatment was abruptly stopped by quenching in water. The nitrogen content of the alloys was determined by micro-Kjeldahl techniques.

X-Ray powder photographs were taken of the arc-melted and of the heat-treated samples in a Guinier focusing camera with strictly monochromatized $\text{CuK}\alpha_1$ radiation and using KCl ($a = 6.2919 \text{ \AA}$ at 20°C) as an internal standard.

The densities were obtained from the loss of weight in benzene.

Table 1. Unit cell dimensions of the α -titanium solid solutions in alloys TiN_x heat-treated at 900°C for 1 month.

x	a Å	c Å	c/a	V Å ³	
0	2.9506	4.6788	1.5857	35.28 (8)	
0.07	2.959	4.739	1.602	35.93	
0.12	2.9621	4.7547	1.6052	36.13	
0.16	2.9681	4.7732	1.6082	36.42	
0.22	2.9711	4.7843	1.6103	36.57	(two-phase region)
0.32	2.9723	4.7862	1.6103	36.62	» »

Table 2. Unit cell dimensions of the tetragonal ϵ phase in alloys TiN_x heat-treated at 900°C for 1 month.

x	a Å	c Å	c/a	V Å ³	d_{obs} g/ml	d_{calc} g/ml	
0.32	4.9414	3.0375	0.6147	74.17	4.76	—	(two-phase region)
0.49	4.9428	3.0357	0.6141	74.17	4.86	4.90	
0.52	4.9452	3.0342	0.6136	74.21	4.86	4.91 *	» »

* for the limiting composition $\text{TiN}_{0.50}$.

Table 3. Unit cell dimensions of the cubic TiN phase in alloys TiN_x heat-treated at 900°C for 1 month.

x	a Å	V Å ³	d_{obs} g/ml	d_{calc} g/ml	
0.52	4.224	75.36	4.86	—	(two-phase region)
0.61	4.2238	75.35	4.95	(4.97) *	» »
0.71	4.2259	75.47	5.02	5.09 *	

* assuming 100 % occupancy of the metal atom sites.

RESULT OF THE PHASE ANALYSIS

The powder patterns of the samples annealed at 900°C were throughout of good quality showing sharp reflexions. For compositions TiN_x with $x < 0.2$, only lines corresponding to the α -titanium solid solution were present. For higher x values, this was followed by a two-phase region. The additional system of lines, which was found to be in agreement with that of the ϵ phase reported by Palty *et al.*⁵, was free from extra lines at the composition $\text{TiN}_{0.5}$. At still higher nitrogen contents, the ϵ phase was contaminated by the TiN phase which was the only phase present above the composition $\text{TiN}_{0.6}$. The general appearance of the system at 900°C is thus in accordance with the findings of Palty *et al.*

The unit cell dimensions of the three phases in the various samples are listed in Tables 1—3. The indexing of the ϵ phase powder pattern was possible assuming a primitiv tetragonal unit cell (*cf.* Table 4).

For the α region, the maximum solubility of nitrogen at 900°C was found to correspond to the composition $\text{TiN}_{0.20}$ (*cf.* Fig. 1). No lines except those of a *hcp* metal atom arrangement were observed, which was taken as evidence

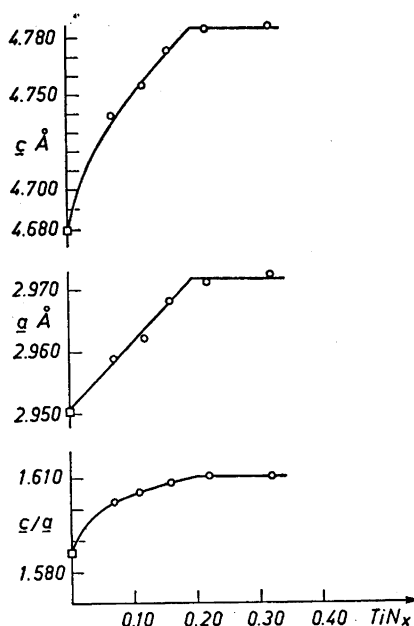


Fig. 1. Lattice parameters of α -titanium solid solutions in alloys TiN_x heat-treated at 900°C.

that the nitrogen atoms occupy interstitial positions in a random way. The mechanism of solubility is evidently the same as the one previously demonstrated in the Hf—O system³ and for lower contents of oxygen in the Ti—O and Zr—O system^{1,2}. The incorporation of the nitrogen atoms causes a continuous increase of both the a and c axes of the titanium lattice.

The ϵ phase seems to exist over a relatively narrow range of homogeneity close to the composition $TiN_{0.5}$. Some evidence, which is however not considered as conclusive, indicates that the maximum content of nitrogen is at $TiN_{0.50}$. Structural data for this phase are given below.

The lower limit of the nitrogen content of the TiN phase was found to be at $TiN_{0.6}$ for the 900°C samples.

The powder patterns of the samples obtained by quenching from the melt in the arc furnace generally showed rather diffuse reflexions. The displacement of the lines indicated that the ranges of homogeneity exceed the value $x = 0.20$ for the α phase and are below $x = 0.6$ for the TiN phase. These observations are in agreement with those of previous authors. No extra reflexions were found in the α phase pattern. The diffuse character of the photographs should, however, make it difficult to observe such weak reflexions. Thus the present findings are not in conflict with the statement by Nowotny *et al.*⁶ that a state of order similar to that of an *anti*-CdI₂ structure should be present in high-temperature samples of the composition $TiN_{0.25}$. Very weak lines correspond-

Table 4. Guinier powder pattern of Ti_2N . Dimensions of the tetragonal unit cell: $a = 4.9452 \text{ \AA}$, $c = 3.0342 \text{ \AA}$.

I	$\sin^2\Theta_{\text{obs}}$	hkl	$\sin^2\Theta_{\text{calc}}$
w	0.04849	110	0.04852
vw	0.08872	101	0.08870
st	0.09700	200	0.09704
vst	0.11296	111	0.11296
m	0.12137	210	0.12130
m	0.18567	211	0.18574
m	0.19401	220	0.19408
m	0.25774	002	0.25776
st	0.28286	301	0.28278
st	0.30712	311	0.30704
vw	0.31576	320	0.31538
m	0.35475	202	0.35480
m	0.37918	212	0.37906
m	0.37991	321	0.37982

ing to the principal reflexions of the ε phase were observed in some non-equilibrium samples quenched in the arc furnace. This seems to indicate that this phase, although not stable at high temperatures, forms rapidly upon passing its maximum temperature of existence.

THE CRYSTAL STRUCTURE OF Ti_2N

Complete single crystal data for Ti_2N were obtained from Weissenberg photographs taken around $[001]$ and $[101]$ of a slightly ellipsoidal crystal measuring about 0.03 mm. Multiple film technique was applied and the inten-

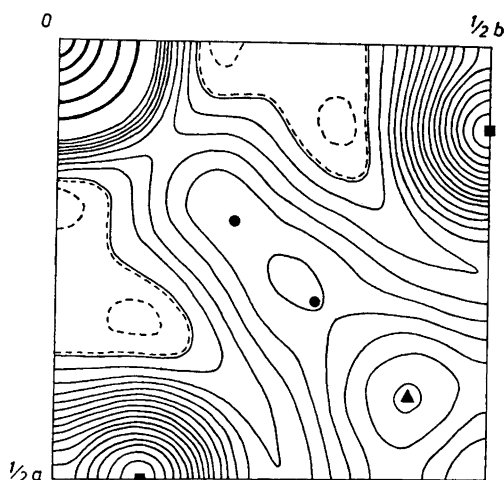


Fig. 2. Patterson projection along $[001]$. \blacktriangle and \blacksquare represent Ti—Ti vectors of multiplicity one and two respectively, while \bullet corresponds to Ti—N vectors of multiplicity two.

Table 5. Comparison of observed and calculated structure factors for Ti_2N .

hkl	$ F _{\text{obs}}$	$ F _{\text{calc}}$	hkl	$ F _{\text{obs}}$	$ F _{\text{calc}}$
200	34.3	38.3	101	10.3	7.6
400	18.4	17.0	301	32.8	34.4
600	5.4	5.5	501	19.4	20.9
110	18.4	16.1	111	36.2 *	49.5
210	28.5	27.8	211	17.1	17.3
310	<7	3.7	311	24.0	22.9
410	25.8	28.1	411	<6	0.1
510	10.0	9.7	511	<5	2.6
220	34.0	37.6	221	13.8	12.1
320	16.6	13.0	321	19.3	17.4
420	8.7	6.3	421	13.8	13.6
520	<6	1.5	521	16.9	20.2
330	22.3	21.7	331	13.0	11.8
430	16.1	15.0	431	10.1	9.8
530	11.0	13.3	531	<3	1.4
440	<7	5.7	441	14.4	16.9

* excluded in the calculation of the reliability index.

sities were estimated visually using a calibrated set of reflexions. A correction for absorption was introduced, the crystal being approximated to a sphere.

The absent reflexions were those characteristic of the space-groups $P4_2nm$, $P4n2$ and $P4_2/mnm$. The appearance of the reciprocal lattice planes $hk0$ and $hk2$ was analogous as was also the case with the registered parts of the two planes $hk1$ and $hk3$.

The appearance of the Patterson projection along $[001]$ is shown in Fig. 2. With a cell content of 2 Ti_2N this function could be completely accounted for by the following atomic arrangement:

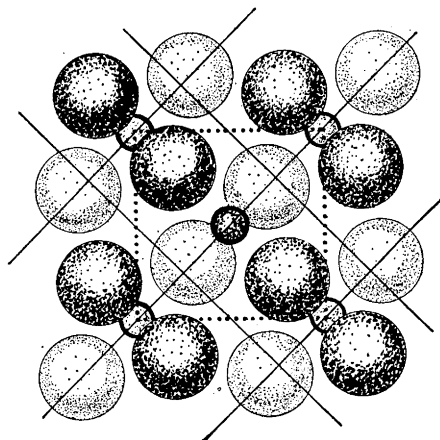


Fig. 3. The crystal structure of Ti_2N projected along the c axis. The large and small circles represent titanium and nitrogen atoms respectively. Light circles have $z = 0$ and dark ones $z = \frac{1}{2}$. The full lines correspond to the β -titanium unit cell.

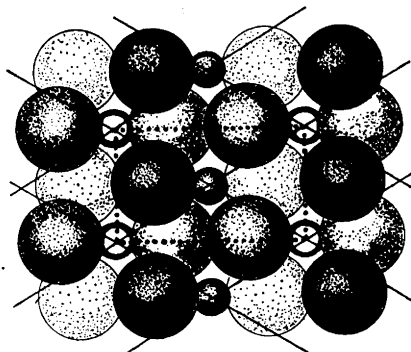


Fig. 4. The crystal structure of Ti_2N projected along the b axis. Large circles represent titanium atoms having $y = 0.204, 0.296, 0.704$ and 0.796 respectively, indicated by increasing darkness. Small circles represent nitrogen atoms, light ones having $y = 0$ and dark ones $y = \frac{1}{2}$. The full lines correspond to the a -titanium unit cell.

Space-group: $P4_2/mnm$ (No. 136)

Unit cell dimensions: $a = 4.9452 \text{ \AA}$, $c = 3.0342 \text{ \AA}$

Unit cell content: 2 Ti_2N

4 Ti in 4(f): $x, x, 0$; $\bar{x}, \bar{x}, 0$; $\frac{1}{2} + x, \frac{1}{2} - x, \frac{1}{2}$; $\frac{1}{2} - x, \frac{1}{2} + x, \frac{1}{2}$

2 N in 2(a): $0, 0, 0$; $\frac{1}{2}, \frac{1}{2}, \frac{1}{2}$

A preliminary value of $x_{\text{Ti}} = 0.30$ was obtained from the Patterson projection.

The refinement of the structure was performed by electron density calculations and also by the method of least squares. An isotropic temperature factor of 1.27 \AA^2 was employed. In this way the following parameter value was obtained:

$$x_{\text{Ti}} = 0.296$$

$$\sigma = \pm 0.001$$

A comparison between the observed and calculated structure factors is given in Table 5. The reliability index, disregarding non-observed reflexions, is 0.094.

The structure thus obtained may be characterized as an *anti*-rutile type. The titanium atoms are arranged to form octahedra that are joined by edges to form strings running parallel to the c axis. Neighbouring strings are joined

Table 6. Comparison of the atomic arrangements around the Ti atoms in β -titanium and Ti_2N .

bcc		Ti_2N
Ti — 4 Ti 3.307 \AA	Ti — 1 Ti 2.853 \AA	(shared edge of Ti_6 octahedron)
	— 2 Ti 3.555	
	— 1 Ti 4.140	(space diagonal of Ti_6 octahedron, a N atom being situated at the centre of this polyhedron)
		(oblique edge of Ti_6 octahedron) (c direction)
— 8 Ti 2.864	— 8 Ti 2.936	
— 2 Ti 3.307	— 2 Ti 3.034	
	— 1 N 2.070	
	— 2 N 2.082	

Table 7. Comparison of the atomic arrangements around the Ti atoms in α -titanium ($\text{TiN}_{0.10}$), Ti_2O and Ti_2N .

$hcp (\text{TiN}_{0.10})$			Ti_2O			Ti_2N		
Ti	— 6 Ti	2.972 Å	Ti	— 6 Ti	2.960 Å	Ti	— 2 Ti	3.034 Å
	— 6 Ti	2.944		— 3 Ti	2.860		— 4 Ti	2.936
				— 3 Ti	3.066		— 1 Ti	2.853
							— 4 Ti	2.936
	— 6 Ti	4.183		— 3 Ti	4.116		— 1 Ti	3.555
				— 3 Ti	4.262		— 1 Ti	3.555
							— 1 Ti	4.140
							— 2 Ti	4.165
	— 6 x N	2.092		— 3 O	2.131		— 2 Ti	4.674
							— 1 N	2.070
							— 2 N	2.082

mutually by sharing corners. The nitrogen positions are at the centers of the titanium octahedra. The structure is illustrated in Figs. 3 and 4. In the former figure, representing the projection parallel to [001], the relation of Ti_2N to the *bcc* metal structure is demonstrated. The presence of nitrogen atoms in the Ti_2N phase at sites corresponding to the $\frac{1}{2}00$ or $\frac{1}{2}0\frac{1}{2}$ positions of the *bcc* lattice causes the distortion of the latter shown in Table 6.

The projection parallel to [010] given in Fig. 4 shows the relation to α -titanium. Half of the face diagonals ($a + c$) of Ti_2N correspond to the a_a (b_a) axes. The metal atom coordinates related to these axes are not $\frac{1}{3}, \frac{2}{3}$ and $\frac{2}{3}, \frac{1}{3}$ but 0.296, 0.704 and 0.704, 0.296. The b axis of Ti_2N corresponds to the c_a axis. In the *hcp* arrangement the atoms form planes $c_a/2$ apart but in Ti_2N the metal atoms are slightly displaced from these planes ($y = 0.250$ and 0.750), y_{Ti} in Ti_2N actually having the values 0.204, 0.296, 0.704 and 0.796.

Table 7 gives a comparison of the atomic arrangements around the Ti atoms in α -titanium, Ti_2O and Ti_2N . Ti_2O has an *anti*- $\text{Cd}(\text{OH})_2$ type of structure, the hexagonal unit cell containing two Ti atoms at $\frac{1}{3}, \frac{2}{3}, z$ and $\frac{2}{3}, \frac{1}{3}, \bar{z}$ with $z = 0.263$ and one O atom at $0,0,0^1$. In this structure the oxygen atoms occupy all the octahedral interstices in every second layer parallel to the *ab* plane while in Ti_2N the nitrogen atoms occupy one half of the octahedral holes in every layer.

Acknowledgement. The author wishes to express his sincere gratitude to Professor A. Ölander for his kind interest and to Professor A. Magnéli for his continuing encouragement and for many valuable discussions.

REFERENCES

1. Holmberg, B. *Acta Chem. Scand.* **16** (1962) 1245.
2. Holmberg, B. and Dagerhamn, T. *Acta Chem. Scand.* **15** (1961) 919.
3. Dagerhamn, T. *Acta Chem. Scand.* **15** (1961) 214.
4. Ehrlich, P. *Z. anorg. Chem.* **259** (1949) 1.
5. Palty, A. E., Margolin, H. and Nielsen, J. P. *Trans. Am. Soc. Metals* **46** (1954) 312.
6. Nowotny, H., Benesovsky, F., Brukl, C. and Schob, O. *Monatsh.* **92** (1961) 403.
7. Hambling, P. G. *Acta Cryst.* **6** (1953) 98.
8. Szántó, I. *Acta Tech. Acad. Sci. Hung.* **13** (1955) 363.

Received December 19, 1961.